NACA

RESEARCH MEMORANDUM

AERODYNAMIC CHARACTERISTICS OF THE NACA RM-10 RESEARCH MISSILE IN THE AMES 1- BY 3-FOOT SUPERSONIC WIND TUNNEL NO. 2 - PRESSURE AND FORCE MEASUREMENTS AT MACH NUMBERS OF 1.52 AND 1.98

By Edward W. Perkins, Forrest E. Gowen, and Leland H. Jorgensen

Ames Aeronautical Laboratory
Moffett Field, Calif.

NATIONAL ADVISORY COMMITTEE FOR AERONAUTICS

WASHINGTON
September 19, 1951

[redacted]

NATIONAL ADVISORY COMMITTEE FOR AERONAUTICS

RESEARCH MEMORANDUM

AERODYNAMIC CHARACTERISTICS OF THE NACA RM-10 RESEARCH MISSILE IN THE AMES 1- BY 3-FOOT SUPERSONIC WIND TUNNEL NO. 2 - PRESSURE AND FORCE MEASUREMENTS AT MACH NUMBERS OF 1.52 AND 1.98

By Edward W. Perkins, Forrest E. Gowen, and Leland H. Jorgensen

SUMMARY

An experimental investigation of the aerodynamic characteristics of a fin-stabilized body of revolution, designated as the RM-10, was made in the NACA Ames 1- by 3-foot supersonic wind tunnel No. 2. Pressure distributions and force characteristics were determined for the body alone at Mach numbers of 1.52 and 1.98. Force characteristics of the body-tail combination were determined at a Mach number of 1.98. Data are presented for Reynolds numbers of 8.6 and 17.4 millions, based on body length.

Of the three theoretical methods used for prediction of the zero-lift pressure distribution for the body alone, the linearized theory of Jones and Margolis (NACA TN 1081) was in best agreement with the experimental distribution over the forebody. Over the afterbody, the magnitudes of the experimental pressure coefficients were in general less than predicted by theory. Except for the aft leeward regions of the body where flow separation occurred at high angles of attack, the distribution of lifting pressure was adequately predicted by inviscid theory. (See, for example, NACA TN 2044.) The variation with angle of attack of the lift, foredrag increment, and center-of-pressure position were much more accurately predicted by the method of Allen (NACA RM A9I26) than by potential theory.

Comparison of the experimental lift, foredrag, and pitching-moment characteristics of the body alone with the results of a similar investigation in the Lewis 8- by 6-foot supersonic wind tunnel (NACA RM E50D10 and NACA RM E50D28) shows that for Mach numbers of 1.52 and 1.98 there is little effect of Reynolds number on these characteristics within the Reynolds number range of 8.6 to 30 millions. Similar comparisons for the

body–tail combination for a Mach number of 1.98 show that, with the exception of the minimum foredrag, the effect on the force and moment characteristics of the increase in Reynolds number from 8.6 million to 30 million is small. The minimum foredrag increases approximately 16 percent with an increase in Reynolds number from 17.4 million to 30 million.

INTRODUCTION

As a part of an integrated program to assess the effects of Reynolds number on aerodynamic characteristics at supersonic speeds, tests are being conducted at various NACA flight and wind–tunnel facilities on a fin–stabilized body of revolution, designated as the RM–10. The first published results of wind–tunnel tests of an RM–10 model were obtained in the 8– by 6–foot supersonic wind tunnel at the Lewis Laboratory at a Reynolds number of 30 million and for a Mach number range of 1.49 to 1.98 (references 1 and 2). The present investigation was conducted in the Ames 1– by 3–foot supersonic wind tunnel No. 2 with an RM–10 model at Reynolds numbers of 8.6 and 17.4 millions and for Mach numbers of 1.52 and 1.98 for the body alone and 1.98 for the body–tail combination.

The purpose of this investigation was to determine the aerodynamic characteristics of the RM–10 configuration within the Mach number and Reynolds number range available and to compare these experimental results with theory and with other experimental results.

NOTATION

A	maximum cross–sectional area of the body, square inches
A_p	body plan–form area, square inches
c	a constant $\left(\frac{R}{l^2}\right)$
c_{d_c}	section drag coefficient of a circular cylinder in terms of the diameter
C_{D_F}	foredrag coefficient $\left(\frac{\text{total drag} - \text{base drag}}{q_o A}\right)$

$\left(C_{D_F}\right)_{\alpha=o}$ foredrag coefficient at 0° angle of attack

ΔC_{D_F} increment of foredrag coefficient $\left[C_{D_F} - \left(C_{D_F}\right)_{\alpha=o}\right]$

C_L lift coefficient $\left(\frac{\text{lift}}{q_o A}\right)$

C_m pitching-moment coefficient about the station of maximum body diameter $\left(\frac{\text{pitching moment}}{q_o A l}\right)$

C_p pressure coefficient $\left(\frac{p-p_o}{q_o}\right)$

$\left(C_p\right)_{\alpha=o}$ pressure coefficient at 0° angle of attack

ΔC_p lifting-pressure coefficient $\left[C_p - \left(C_p\right)_{\alpha=o}\right]$

L length of the body, inches

l axial distance from the body nose to the maximum body diameter station, inches

M_o free-stream Mach number

p local static pressure, pounds per square inch

p_o free-stream static pressure, pounds per square inch

q_o free-stream dynamic pressure $\left(\frac{\gamma}{2} p_o M_o^2\right)$, pounds per square inch

r local body radius at a station x distance from the nose, inches

R maximum body radius, inches

[redacted]

[redacted]

Re	free-stream Reynolds number based on body length
S_b	cross-sectional area of the base of the body, square inches
x	distance from the nose measured along the longitudinal body axis, inches
x_m	distance from the nose to the center of moments, inches
x_p	distance from the nose to the centroid of the plan-form area, inches
vol	total volume of the body, cubic inches
α	angle of attack, degrees
γ	ratio of the specific heats of air, taken as 1.40
η	ratio of the drag coefficient of a circular cylinder of finite length to that of a cylinder of infinite length
θ	body cylindrical coordinate, degrees

APPARATUS

This investigation was conducted in the Ames 1- by 3-foot supersonic wind tunnel No. 2, which is an intermittent-operation, nonreturn, variable-pressure wind tunnel. The high-pressure air is obtained from the Ames 12-foot wind tunnel at a pressure of about six atmospheres and is expanded through the nozzle to the atmosphere. A change in Reynolds number is obtained by varying the total pressure by means of a butterfly valve between the two tunnels. The nozzle is equipped with flexible top and bottom plates which can be shaped to give test-section Mach numbers in the range of 1.2 to 4.0. The strain-gage balance and other tunnel instrumentation used in this investigation are described in detail in reference 3. However, for this investigation the pitching moments were measured by means of a strain gage mounted on the supporting sting rather than by the method described in reference 3.

A sketch of the 1/12-scale RM-10 missile, giving the important model dimensions and the equation for the parabolic-arc profile, is shown in figure 1. The fineness ratio of the closed body of revolution is 15; however, to provide for the rocket jet in the free-flight models and sting mounting of the wind-tunnel models, the base was cut off at the

81.5-percent-length station, which resulted in a fineness ratio of 12.2. The two model configurations tested were the body alone and the body-tail combination shown in figure 1.

TESTS

The testing program was divided into three parts, and the test conditions for each of these parts are listed in the following table:

Test	M_o	Average Re (millions)	α (deg)
Pressure distribution, body alone	1.52	8.6	0 to 15
	1.52	17.4	0
	1.98	8.6	0 to 5-1/2
Force tests, body alone	1.52	8.6 and 17.4	0 to 14
	1.98	8.6	0 to 14
Force tests, body-tail combination	1.98	8.6 and 17.4	0 to 6

The static-pressure distributions were measured at 30° increments in circumferential angle with a single longitudinal row of orifices on the model by rotating the model about its axis. Force-test results for the body-tail combination at a Mach number of 1.52 have not been presented because of unknown interference effects on the tail surfaces due to the shock wave from the sting support and the reflected bow wave.

REDUCTION OF DATA

Corrections to Experimental Results

All of the experimental data have been reduced to coefficient form and have been corrected for the effects of the nonuniform flow conditions existing in the wind tunnel. The free-stream static-pressure variations in the empty tunnel have been applied as corrections to the body pressure-distribution data by simple linear superposition. Corrections to pressure-distribution data due to the effect of stream-angle variation were within the limits of accuracy of the data and have therefore been neglected.

The corrections to the force tests have been calculated by the method of reference 4, in which the stream angle and pressure distribution in the vertical plane of symmetry of the empty tunnel are used. The average magnitudes of the total corrections to C_L, C_m, and C_{D_F} due to stream flow nonuniformities are tabulated as follows:

Mach number	Coefficient	Body alone	Body–tail combination
1.52	C_L	0.02	– – –
	C_m	.002	– – –
	C_{D_F}	.007	– – –
1.98	C_L	.02	0.03
	C_m	.002	.01
	C_{D_F}	.009	.003

Precision of Results

The precision of the experimental data was calculated from estimates of the uncertainty or possible error in the individual measurements which entered into the determination of the angle of attack, the stream characteristics, and the aerodynamic coefficients. The probable uncertainty in the final results was determined by the method given in reference 5. The uncertainties in the lift, pitching-moment, foredrag, and pressure coefficients are tabulated as follows:

Coefficient	Body alone	Body–tail combination
C_L	±0.018	±0.030
C_m	±.010	±.012
C_{D_F}	±.006	±.006
C_p	±.005	– – –

The error in the angle-of-attack measurements is not greater than $\pm 0.15^\circ$. The free-stream Mach number, M_o, is known accurately within ±0.005 at a given point in the stream; however, the variation of Mach number along the body axis was as much as ±0.02. Due to the fairly high rate of decrease in wind-tunnel stagnation temperature with tunnel operating time, the variation in Reynolds number during each run was approximately $\pm 0.7 \times 10^6$ at both Mach numbers.

RESULTS AND DISCUSSION

Pressure Distributions

The theoretical and experimental longitudinal distributions of pressure coefficient for the body alone at zero angle of attack are shown in figure 2. The experimental data from reference 1 are included for comparison. Three theoretical curves based on the linearized theory of reference 6, the second-order theory of reference 7, and the method of characteristics (see, e.g., reference 8) are also shown for comparison. It was noted in reference 1 that the experimental results obtained in that investigation were in good agreement with the distribution predicted by the theoretical expression developed in the report.[1] For the present investigation, the distribution predicted by the linearized theory (reference 6) is in best agreement with the experimental distribution for the forward 50 percent of the body length. Over the afterbody the magnitudes of the experimental pressure coefficients are, in general, less than predicted by any of the theories. Due to inherent experimental uncertainties involved in the data from both sources (the present investigation and reference 1), and because the differences in the theoretical results are small, no statement can be made as to which of the theories is the best for all of the test conditions.

As predicted by theory, an increase in Mach number results in a decrease in pressure coefficient over the forward 30 percent of the body length. Aft of the 30-percent point, although theory predicts a decrease in the magnitude of the pressure coefficient with increase in Mach number, no conclusion can be drawn from the experimental data in this region because of the uncertainty in the individual pressure measurements.

The theoretical and experimental circumferential distributions of lifting-pressure coefficient for three angles of attack and six axial length stations are presented in figure 3. The theoretical curves shown in this figure are based on the second-order theory of reference 7.[2] For stations forward of the maximum thickness, and at an angle of attack of 5.5°, the theoretical pressure recovery over the lee side of the body is small, and the agreement between theory and experiment is good. As the angle of attack is increased to 11° or to 15°, the theoretical pressure recovery increases, and the experimental data show a pressure recovery somewhat less than theory, indicating a large region of

[1] The expression for the zero-lift pressure distribution developed independently by Luidens and Simon in reference 1 is identical with the result presented in reference 7.

[2] The equations for lifting-pressure distribution obtained from references 1, 7, and 9 are identical to the order α^2.

separated flow on the lee side of the body. For stations aft of the maximum thickness, the theoretical pressure recovery on the lee side of the body is large and the experimental data indicate the presence of a separated region even at an angle of attack of 5.5°. This separated region becomes progressively larger with increase in angle of attack and distance aft of the maximum thickness point. At the most rearward position, the separated region extends even past the 90° point to the windward side of the model. (See fig. 3(f).)

The lifting-pressure distribution results of reference 1 are in good agreement with those of the present investigation; however, none of the data from reference 1 have been included in figure 3 as those data were obtained at slightly different angles of attack and different x/L stations. Since the tests of that reference were made for the same Mach number range, but for a Reynolds number of approximately 30 million as compared to 8.6 million for the data of this investigation, it may be concluded that any effects of Reynolds number on the lifting pressures are small within the 9° angle-of-attack range for which comparisons can be made. It has been shown in reference 2 that there is an increase in lift with increase in Mach number; however, the pressure-distribution data of reference 1 and the present investigation do not show any consistent change in lifting-pressure coefficients with Mach number. This anomaly probably results from the fact that within this low angle-of-attack range the increase in lift is small, and consequently the accompanying change in local pressure coefficient is within the uncertainty of the data. However, it cannot be concluded from these comparisons that there are no appreciable Mach number effects on local lifting-pressure coefficient at angles of attack above 9° because, as will be shown later, the effect of Mach number on lift increased markedly above an angle of attack of 10° or 12° for the test conditions of the present investigation.

Body-Alone Force Tests

The variations of the aerodynamic coefficients and center-of-pressure position with angle of attack for the body alone are presented in figures 4 through 8. For comparison with these experimental results, theoretical curves based on the linearized potential theory of reference 10 and the theory of reference 11 are shown.

The linearized theory neglects any effects of viscosity and considers only the potential flow. The theory of reference 11 has been developed considering the effects of viscosity on the cross flow for inclined bodies of revolution, and the resulting equations for the aerodynamic coefficients at moderate angles of attack are as follows:

$$C_L = 2\left(\frac{S_b}{A}\right)\alpha + \eta\, c_{d_c}\left(\frac{A_p}{A}\right)\alpha^2 \tag{1}$$

$$\Delta C_{D_F} = C_{D_F} - (C_{D_F})_{\alpha=0} = \left(\frac{S_b}{A}\right)\alpha^2 + \eta\, c_{d_c}\left(\frac{A_p}{A}\right)\alpha^3 \tag{2}$$

$$C_m = 2\left[\frac{\text{vol}-S_b(L-X_m)}{AL}\right]\alpha + \eta\, c_{d_c}\left(\frac{A_p}{A}\right)\left(\frac{X_m-X_p}{L}\right)\alpha^2 \tag{3}$$

The first term in each equation is the linearized potential theory result, and the second term is the cross force resulting from a consideration of the effects of viscosity on the flow perpendicular to the body axis. In these equations, the numerical value of η depends primarily on the length-to-diameter ratio of the body and was essentially constant ($\eta = 0.7$) for the test conditions of the present investigation. The value of c_{d_c} depends on the Reynolds number and Mach number normal to the axis of the body of revolution; therefore, the dependence of c_{d_c} on free-stream Reynolds number and Mach number is through Re sin α and M_o sin α. For the Reynolds numbers of this investigation, no effect of Reynolds number on the cross-flow drag coefficient has been considered. For the tests at a Mach number of 1.52, the Mach number normal to the axis of revolution was always less than 0.4; hence, in the calculations c_{d_c} was considered constant and equal to 1.2 throughout the angle of attack range. However, for the test at a Mach number of 1.98, the normal Mach number (M_o sin α) exceeded 0.4 at an angle of attack of approximately 12°. Therefore, the value of c_{d_c} used in the calculations increased from 1.2 at 12° to 1.35 at 15°. (See reference 11.) Within this angle-of-attack range, 12° to 15°, the difference in the value of c_{d_c} for the two different free-stream Mach numbers results in the divergence of the force characteristics shown by the theoretical curves in figures 4, 5, 6, and 8.

Lift.- The experimental lift results (fig. 4) for the body alone show reasonable agreement with the curve predicted by the theory of reference 11. However, throughout most of the angle-of-attack range the magnitude of the experimental lift is greater than predicted. At 12° angle of attack, the lift is 8 percent and 13 percent greater than the theoretical values at Mach numbers of 1.52 and 1.98, respectively. At this angle of attack, potential theory underestimate the lift by approximately 70 percent. For angles of attack greater than 12° at a Mach number of 1.98, the experimental data show an increase in lift with increase in M_o sin α as predicted by the theory, although the magnitude of the increase is greater than predicted.

A comparison of the data from reference 2 with that of the present investigation indicates that at a Mach number of 1.98 there is no

Reynolds number effect in the range of 8.6 million to 31.1 million. However, for a Mach number of 1.5, there is a decrease in lift with increase in Reynolds number from 8.6 million to 17.4 million but no further change within the Reynolds number range of 17.4 million to 29.1 million. In the higher angle-of-attack range, above 12°, the Mach number 1.5 results of the present investigation indicate an effect opposite to that noted in the lower angle-of-attack range, that is, an increase in lift with an increase in Reynolds number from 8.6 million to 17.4 million.

Pitching moment.- Contrary to the results obtained by comparison of the theoretical and experimental lift characteristics, potential theory yields a pitching-moment curve which is in closer agreement with experimental results than is the curve for the theory of reference 11. (See fig. 5.) However, since both the lift and, as will be shown later, the center of pressure are unsatisfactorily predicted by potential theory, it is apparent that the agreement of the pitching moments must be considered fortuitous.

The data of reference 2 were obtained for a Mach number range of 1.49 to 1.98 at a Reynolds number of 30 million. For those tests the critical cross-flow Reynolds number based on the maximum body diameter was exceeded at an angle of attack of about 4°. The critical cross-flow Mach number was not exceeded since the angle-of-attack range was limited to 9° and $M_o \sin \alpha$ was therefore less than 0.4. The experimental data obtained for these test conditions did not show any of the unusual variations in the aerodynamic forces which might have been expected as a result of exceeding the critical cross-flow Reynolds number. The data of the present investigation were obtained for a range of test conditions wherein both the critical cross-flow Reynolds number and critical cross-flow Mach number were exceeded. Since the theory of reference 11 predicts variations in pitching moment due to either of these effects, it might be expected that certain unusual variations in pitching moment could result when both were exceeded. The experimental trends shown in figure 5 cannot be explained on the basis of the simple effects of either cross-flow Reynolds number or cross-flow Mach number. It should be mentioned that a combination of Mach number and Reynolds number effects appear to have an influence different from that predicted by theory (reference 12).

In contrast to the results from reference 2, experimental results from the tests of this investigation show an increase in pitching moment with increase in Mach number at angles of attack above about 4°. At angles of attack below 4° any effects due to Mach number are within the experimental uncertainty.

Center of pressure.- The variation of the position of the center of pressure with angle of attack for the body alone is shown in figure 6. Comparison between theory and experiment indicates that the center of

pressure predicted by potential theory is obviously in error at all angles of attack. Much better agreement with experiment is obtained from the theory of reference 11. The center of pressure predicted by this latter theory is about two body diameters ahead of the experimental center of pressure over an angle-of-attack range of 3° to 14°, whereas potential theory predicts a center of pressure which does not vary with angle of attack and is 13-body diameters ahead of the experimental position at 14° angle of attack. The experimental data show no discernible Mach number effect but do, however, show a forward shift of the center-of-pressure position with increase in Reynolds number in the low angle-of-attack range.

The experimental data from reference 2 are in good agreement with the center-of-pressure data from this investigation, but the results of that reference indicate a small rearward shift of center of pressure with increasing Mach number.

Foredrag.- The foredrag results for the body are presented in figure 7. Experimental values of minimum pressure drag and skin-friction drag at 0° angle of attack are presented in the following table for comparison with corresponding theoretical results calculated by several different methods.

Minimum foredrag results

Mach number	1.52	1.52	1.98
Reynolds number - millions	8.6	17.4	8.6
1. Experimental minimum C_{D_F}	.115	.126	.115
Pressure drag coefficients			
2. Linear theory	.051	.051	.048
3. Method of characteristics	.045	.045	.040
4. Experiment	.050	.050	.043
Skin-friction drag coefficients			
5. Laminar incompressible	.016	.012	.016
6. Turbulent compressible (von Kármán, reference 13)	.084	.074	.065
7. Turbulent compressible (Wilson, reference 14)	.096	.085	.087
8. Experiment [(1)-(4)]	.065	.076	.072

A comparison of the experimental and theoretical pressure drags on the body shows that the experimental values of the pressure drag agree with linear theory at a Mach number of 1.52. However, at a Mach number of 1.98 the pressure drag calculated from linear theory is about 10 percent too high.

The theoretical skin-friction drag coefficients shown in the above table were based on flat-plate skin-friction coefficients and were

calculated with the assumption that completely laminar or completely turbulent boundary-layer flow existed on the body. The experimental skin-friction coefficient was obtained as the difference between the experimental foredrag and pressure-drag coefficients. For the lower Reynolds number tests at a Mach number of 1.52, it is apparent that a laminar boundary layer existed over an appreciable portion of the body surface since the most optimistic theoretical estimate of the turbulent skin-friction drag coefficient (reference 13) was considerably greater than the experimental result. An increase in Reynolds number at this Mach number was accompanied by an increase in the skin-friction drag coefficient. Had the boundary layer been completely turbulent at the lower Reynolds number, the skin-friction drag coefficient would have decreased with increasing Reynolds number. Hence, the increase in skin-friction drag coefficient that was observed must have resulted from upstream movement of the transition point, with the result that at higher Reynolds numbers a larger portion of the body surface was subject to turbulent boundary-layer flow. No conclusion can be stated with regard to the correct theoretical value for the skin-friction drag coefficient nor the Reynolds number of transition because of the unknown effects of the free-stream turbulence level and the nonuniformities of the air stream. Since it is believed that an appreciable amount of laminar-boundary-layer flow existed on the model for the higher Reynolds number tests at a Mach number of 1.52, the agreement of von Kármán's turbulent, compressible skin-friction coefficients with experiment is considered fortuitous. Other investigators (e.g., Wilson in reference 14) have found that the values of skin-friction coefficient obtained from von Kármán's turbulent compressible flow equation are lower than experimental values.

The experimental results of the present investigation show no perceptible change in minimum foredrag coefficient with increase in Mach number, but as would be expected with partly laminar-flow conditions there was an increase in minimum foredrag coefficient with increase in Reynolds number from 8.6 to 17.4 millions. Comparison of these results with the results from reference 2 for a Reynolds number of 30 million shows no difference in minimum foredrag coefficient at Reynolds numbers of 17.4 and 30 millions.

The theoretical and experimental results for the increment of foredrag due to angle of attack are presented in figure 8. As expected, the agreement between the theoretical and experimental drag rise was similar to that obtained for the lift in figure 4. These results are also in agreement with the foredrag-rise results from reference 2.

Body-Tail Combination Force Tests

Lift.- The experimental and theoretical lift characteristics for this configuration are shown in figure 9. The theoretical lift of the body-tail combination was calculated by adding the lift due to the body alone to that due to the tail alone with no consideration being given to interference effects. The lift due to the body alone and the tail alone was calculated by the methods of references 11 and 15, respectively. Two theoretical curves are shown. The curve which predicts the higher lift was obtained by assuming the area of the tail enclosed within the body to be fully effective in lift, and the second theoretical curve results from assuming only the exposed surfaces to be effective. The data of figure 9 show that neither assumption is correct; however, the experimental data is bracketed by these theoretical curves.

Theory indicates a small increase in lift-curve slope with increase in angle of attack, but the experimental lift-curve slope was essentially constant throughout the angle-of-attack range. These lift results for test Reynolds numbers of 8.6 million and 17.4 million are in agreement with the results from reference 2 at a Reynolds number of 30 million, with the exception that the data of that report do show a small increase in lift-curve slope with increasing angle of attack similar to that predicted by theory.

Pitching moment and center of pressure.- The variations of pitching moment and center of pressure with angle of attack are shown in figures 10 and 11. Theoretical values of the pitching moment were not calculated because of the uncertainty of the center-of-pressure position for the tail surfaces in the presence of the body.

The slope of the pitching-moment curve of figure 10 is constant throughout the angle-of-attack range. The center-of-pressure position (fig. 11) is constant for all angles of attack and is located 10.3 diameters behind the nose of the missile. These results are in good agreement with the data from reference 2, and any deviations in pitching moment or center of pressure are small and within the uncertainty of the data.

From a comparison of the results of this investigation with those from reference 2 it may be concluded that any effects of Reynolds number are small within the range of Reynolds numbers from 8.6 million to 30 million.

Foredrag.- The variations in foredrag coefficient and increment of foredrag coefficient due to angle of attack are shown in figures 12 and 13. The theoretical rise in foredrag coefficient due to lift was calculated in the same manner as the theoretical lift - that is, by adding the

[redacted]

component due to the body alone to that due to the tail alone. As before, the components were obtained by the methods of references 11 and 15 with the same assumptions regarding the effective tail area being made. In this instance, the assumption that only the exposed tail surfaces are effective in lift yields a good approximation for the drag rise. The data of figures 12 and 13 indicate that any effects of Reynolds number within the range of 8.6 million to 17.4 million are small and within the uncertainty of the data. However, comparison of the drag data of this report with that of reference 2 indicates that there is a Reynolds number effect on minimum foredrag in the range of Reynolds numbers from 17.4 million to 30 million, since the minimum foredrag coefficient obtained in that reference was about 16 percent higher than was obtained in the present investigation. It has been previously shown that there is no apparent Reynolds number effect on the body-alone minimum foredrag coefficient in this range; therefore, the increase in minimum foredrag coefficient must result from a Reynolds number effect on the tail fins and/or the zero-lift interference drag. The increase in the skin-friction drag which would accompany a change from laminar to turbulent flow on the tail fins alone is of the same order of magnitude as the measured difference in minimum foredrag.

SUMMARY OF RESULTS

An investigation of the pressure distribution over the RM-10 body and the aerodynamic force coefficients for the body alone and the body-tail combination was made at Reynolds numbers, based on body length, of 8.6 million and 17.4 million. The test Mach numbers were 1.52 and 1.98 for the body alone and 1.98 for the body-tail combination.

The tests for the body alone indicate the following results:

1. At zero angle of attack, the linear theory of NACA TN 1081 showed good agreement with the experimental pressure distribution over the first 50 percent of the body length. Over the remainder of the body the magnitudes of the pressure coefficients were, in general, less than predicted by any of the theories.

2. Except for the aft leeward regions of the body where separation effects are important at high angles of attack, inviscid theory (see, e.g., NACA TN 2044) was in good agreement with the experimental lifting-pressure distributions.

3. For angles of attack less than 9°, a comparison of the lifting-pressure distribution results of NACA RM E50D10 with the results of this investigation indicated that there were no appreciable Mach number or Reynolds number effects due to an increase in Mach number from 1.52 to

1.98 or an increase in Reynolds number from 8.6 million to 30 million.

4. For the force tests on the body alone, the theory of NACA RM A9I26 showed better agreement with the experimental results than did linearized potential theory. These theoretical results (NACA RM A9I26) agreed well with the experimental lift and foredrag increment at a Mach number of 1.52, but underestimated both at a Mach number of 1.98. This theory overestimated the pitching moment at both Mach numbers but predicted the location and aft movement of the center-of-pressure position with angle of attack much better than did potential theory.

5. For angles of attack less than 9°, a comparison of force data from NACA RM E50D28 with force data from this investigation indicated that any effects on force characteristics due to a change in Reynolds number from 8.6 million to 30 million were small.

The tests for the body-tail combination indicate the following results:

1. For the angle-of-attack range of this test, the lift and pitching moment were linear functions of the angle of attack; hence, the center of pressure remained at a fixed position.

2. Comparison of the results of this investigation with the results of NACA RM E50D28 indicates that, with the exception of minimum foredrag, the effect of Reynolds number on force and moment characteristics was small in the range of Reynolds numbers from 8.6 million to 30 million. The minimum foredrag increased approximately 16 percent with an increase of Reynolds number from 17.4 million to 30 million.

Ames Aeronautical Laboratory
National Advisory Committee for Aeronautics
Moffett Field, Calif.

REFERENCES

1. Luidens, Roger W., and Simon, Paul C.: Aerodynamic Characteristics of NACA RM-10 Missile in 8- by 6-foot Supersonic Wind Tunnel at Mach Numbers from 1.49 to 1.98. I-Presentation and Analysis of Pressure Measurements (Stabilizing fins removed). NACA RM E50D10, 1950.

2. Esenwein, Fred T., Obery, Leonard J., and Schueller, Carl F.: Aerodynamic Characteristics of NACA RM-10 Missile in 8- by 6-foot Supersonic Wind Tunnel at Mach Numbers from 1.49 to 1.98. II - Presentation and Analysis of Force Measurements. NACA RM E50D28, 1950.

3. Van Dyke, Milton D: Aerodynamic Characteristics Including Scale Effect of Several Wings and Bodies Alone and in Combination at a Mach Number of 1.53. NACA RM A6K22, 1946.

4. Nielsen, Jack N., Katzen, Elliott D., and Tang, Kenneth K.: Lift and Pitching-Moment Interference Between a Pointed Cylindrical Body and Triangular Wings of Various Aspect Ratios at Mach Numbers of 1.50 and 2.02. NACA RM A50F06, 1950.

5. Michels, Walter C.: Advanced Electrical Measurements, ch. I, 2d ed., D. Van Nostrand Company Inc., N. Y., 1943.

6. Jones, Robert T., and Margolis, Kenneth: Flow Over a Slender Body of Revolution at Supersonic Velocities. NACA TN 1081, 1945.

7. Lighthill, M. J.: Supersonic Flow Past Slender Pointed Bodies of Revolution at Yaw. Quart. Jour. of Mech. and Appl. Math., vol. 1, pt. 1, Mar. 1948, pp. 76-89.

8. Sauer, Robert: Introduction to Theoretical Gas Dynamics. Trans. by Freeman K. Hill and Ralph A. Alpher. J. W. Edwards Bros., Ann Arbor, Mich., 1947.

9. Allen, H. Julian: Pressure Distribution and Some Effects of Viscosity on Slender Inclined Bodies of Revolution. NACA TN 2044, 1950.

10. Tsien, Hsue-Shen: Supersonic Flow Over an Inclined Body of Revolution. Jour. Aero. Sci., vol. 5, no. 12, Oct. 1938, pp. 480 - 483.

11. Allen, H. Julian: Estimation of the Forces and Moments Acting on Inclined Bodies of Revolution of High Fineness Ratio. NACA RM A9I26, 1949.

12. Allen, H. Julian, and Perkins, Edward W.: Characteristics of Flow Over Inclined Bodies of Revolution. NACA RM A50L07, 1951.

13. von Kármán, Th.: On Laminar and Turbulent Frictions. NACA TM 1092, 1946.

14. Wilson, R. E.: Turbulent Boundary Layer Characteristics at Supersonic Speeds – Theory and Experiment. Univ. of Texas, Defense Research Lab., CM 569, Nov. 1949. (Also available in Jour. Aero. Sci., Sept. 1950, pp. 585–594)

15. Cohen, Doris: The Theoretical Lift of Flat Swept-Back Wings at Supersonic Speeds. NACA TN 1555, 1948.

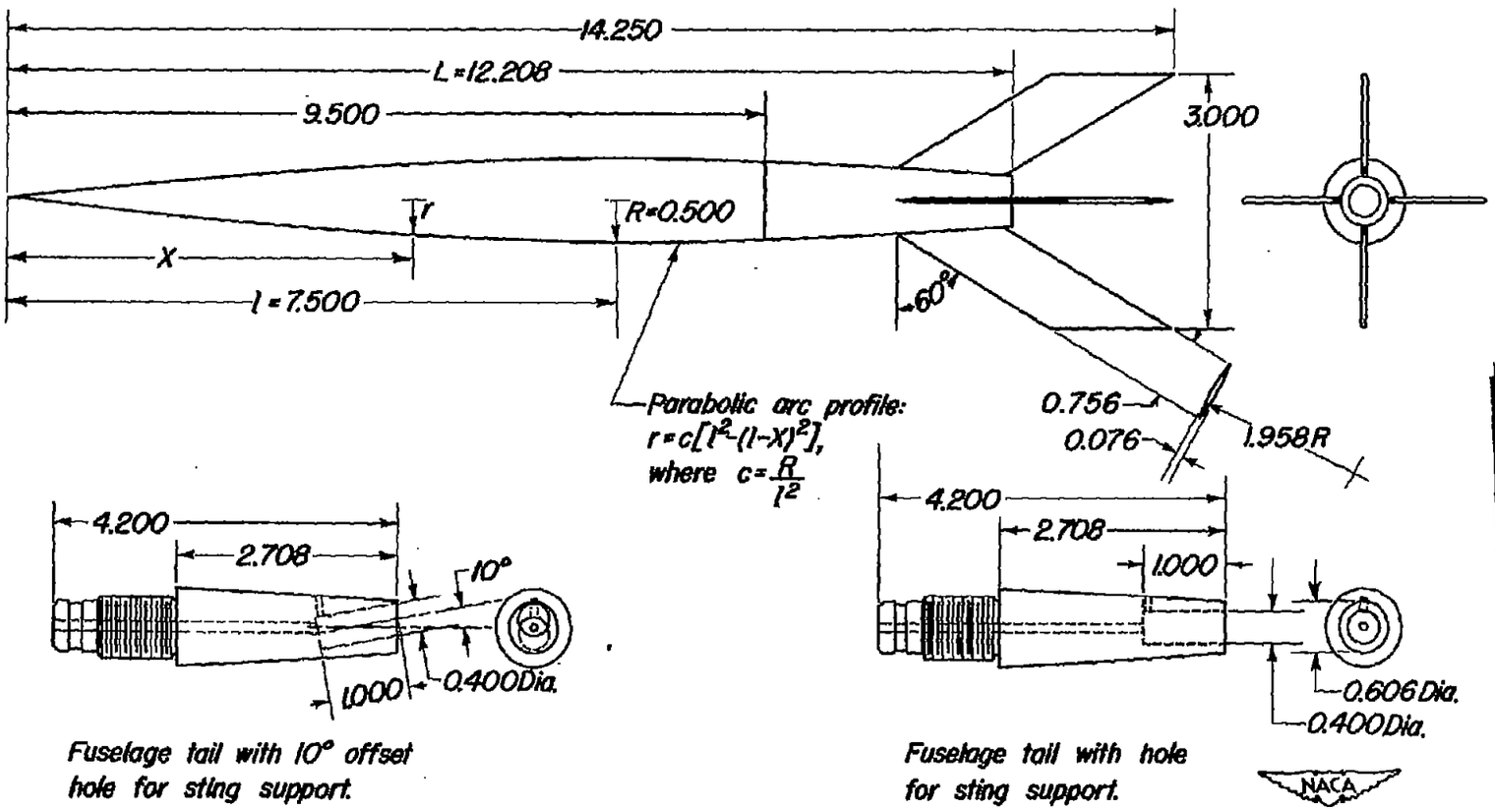

Note: All dimensions are in inches.

Figure 1. – One-twelfth scale RM-10 missile.

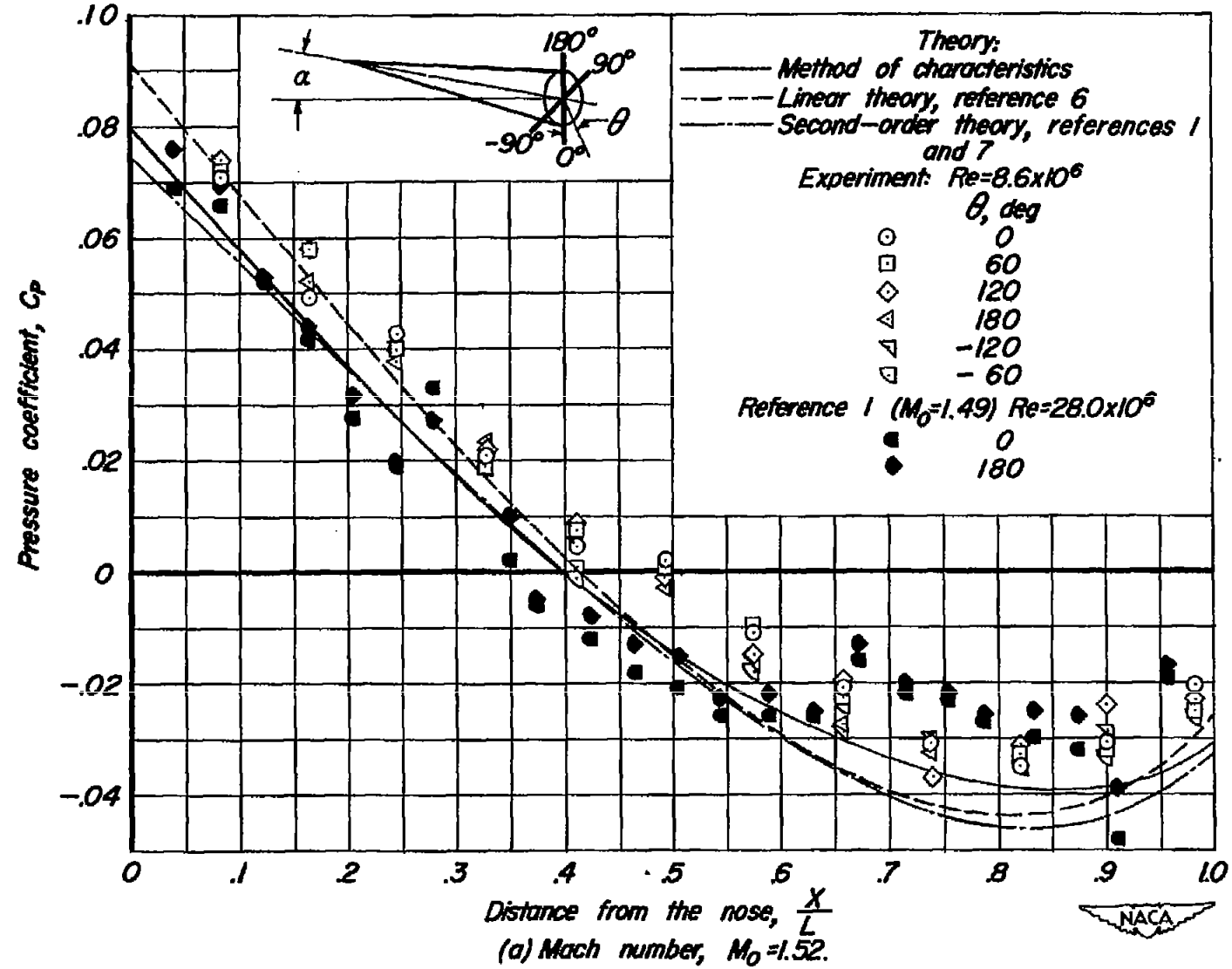

(a) Mach number, M_0 =1.52.

Figure 2. —Longitudinal distribution of pressure coefficient for the body at 0° angle of attack.

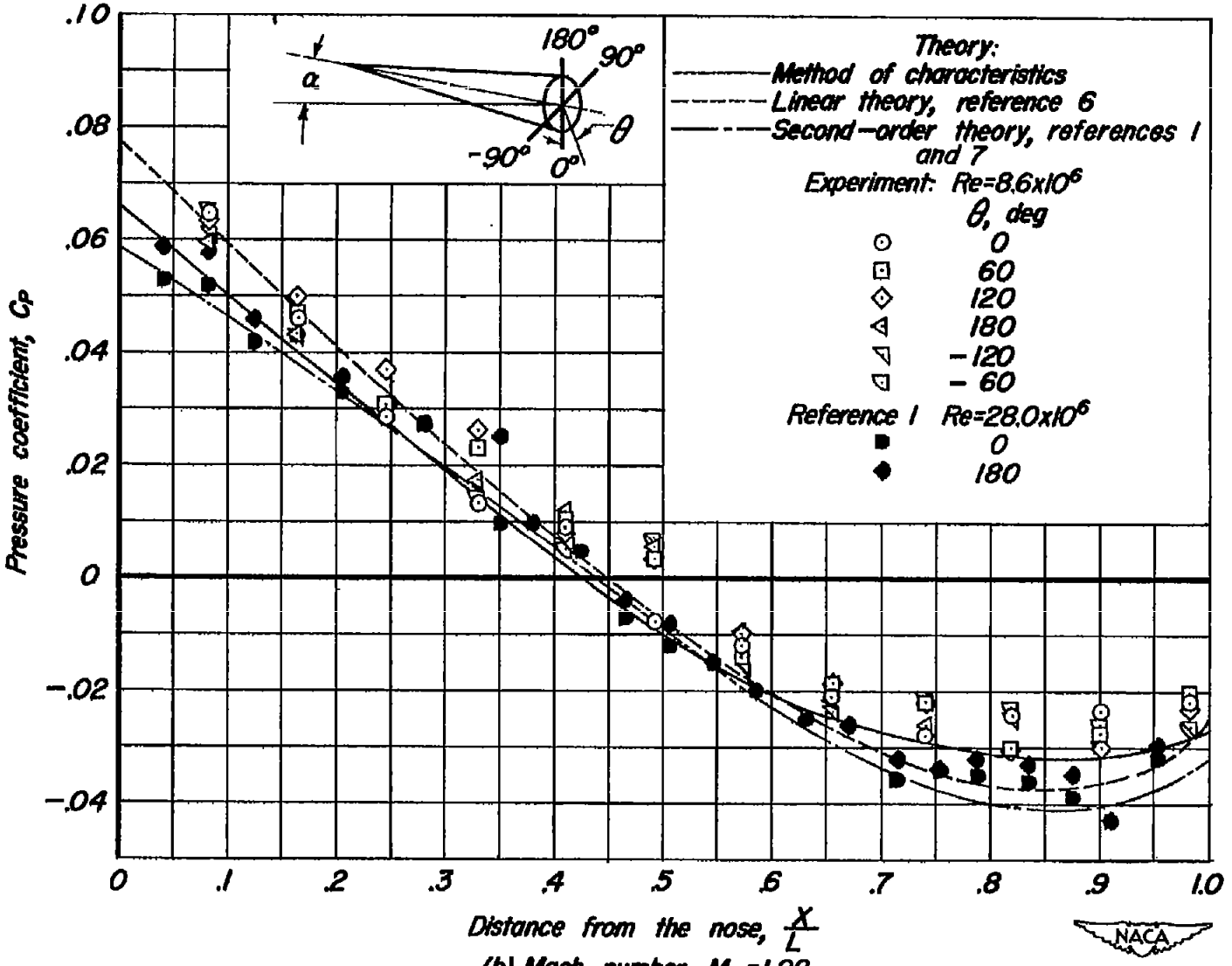

(b) Mach number, $M_0 = 1.98$.

Figure 2.– Concluded.

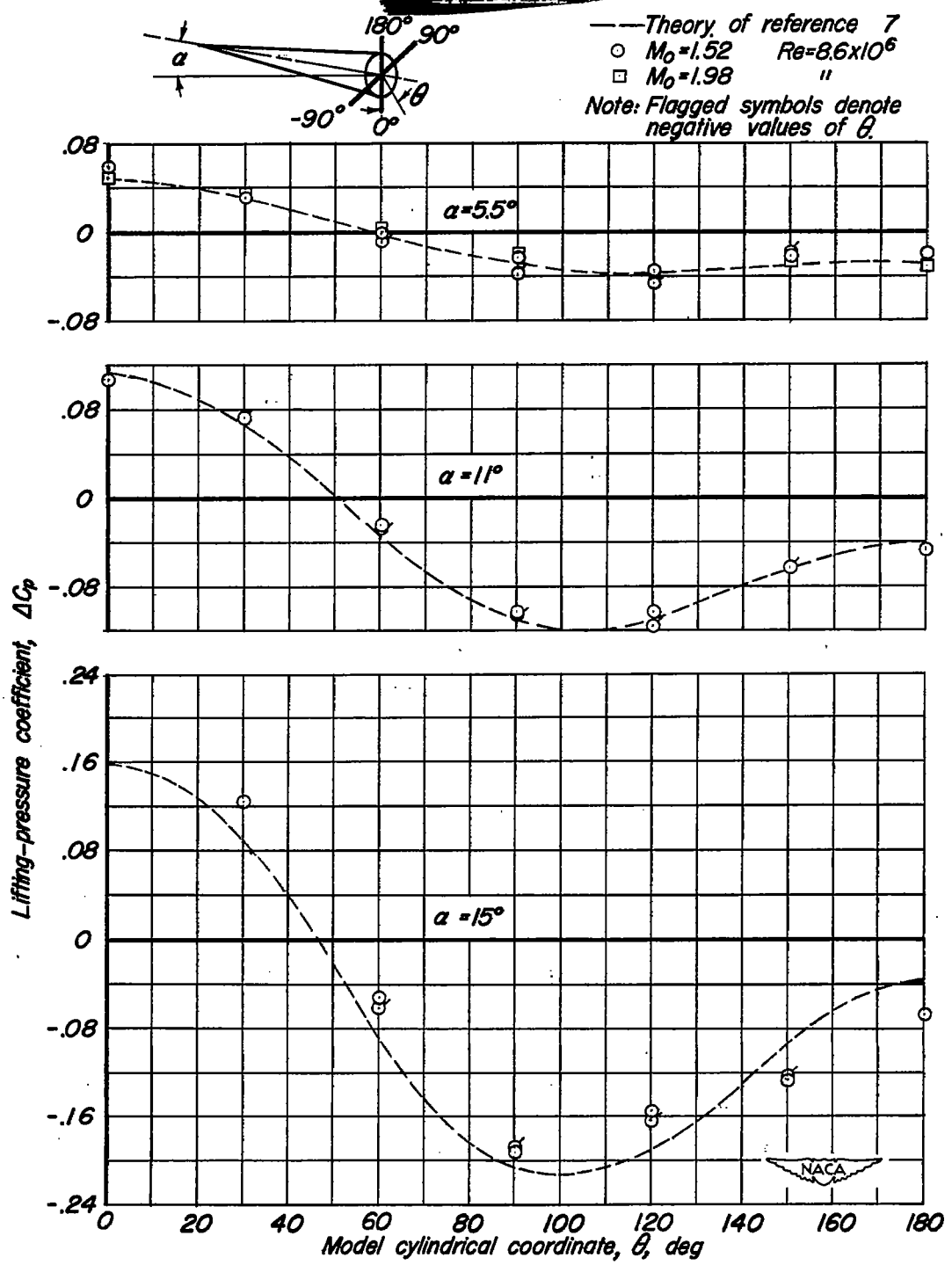

(a) Longitudinal station, $\frac{x}{l}$=0.164.

Figure 3.—Variation of circumferential lifting-pressure coefficient for the body at three angles of attack.

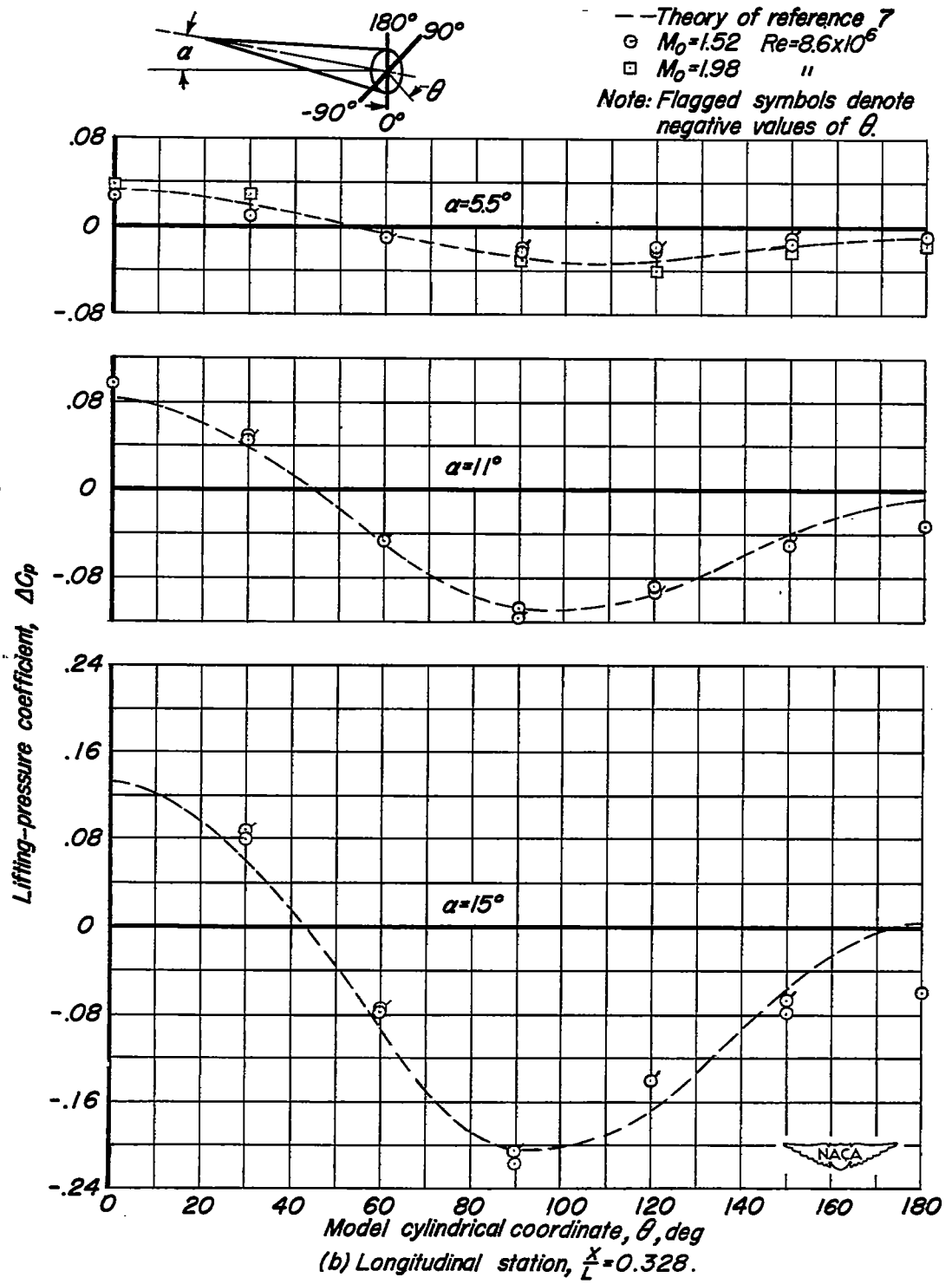

(b) Longitudinal station, $\frac{X}{L}$=0.328.

Figure 3.– Continued.

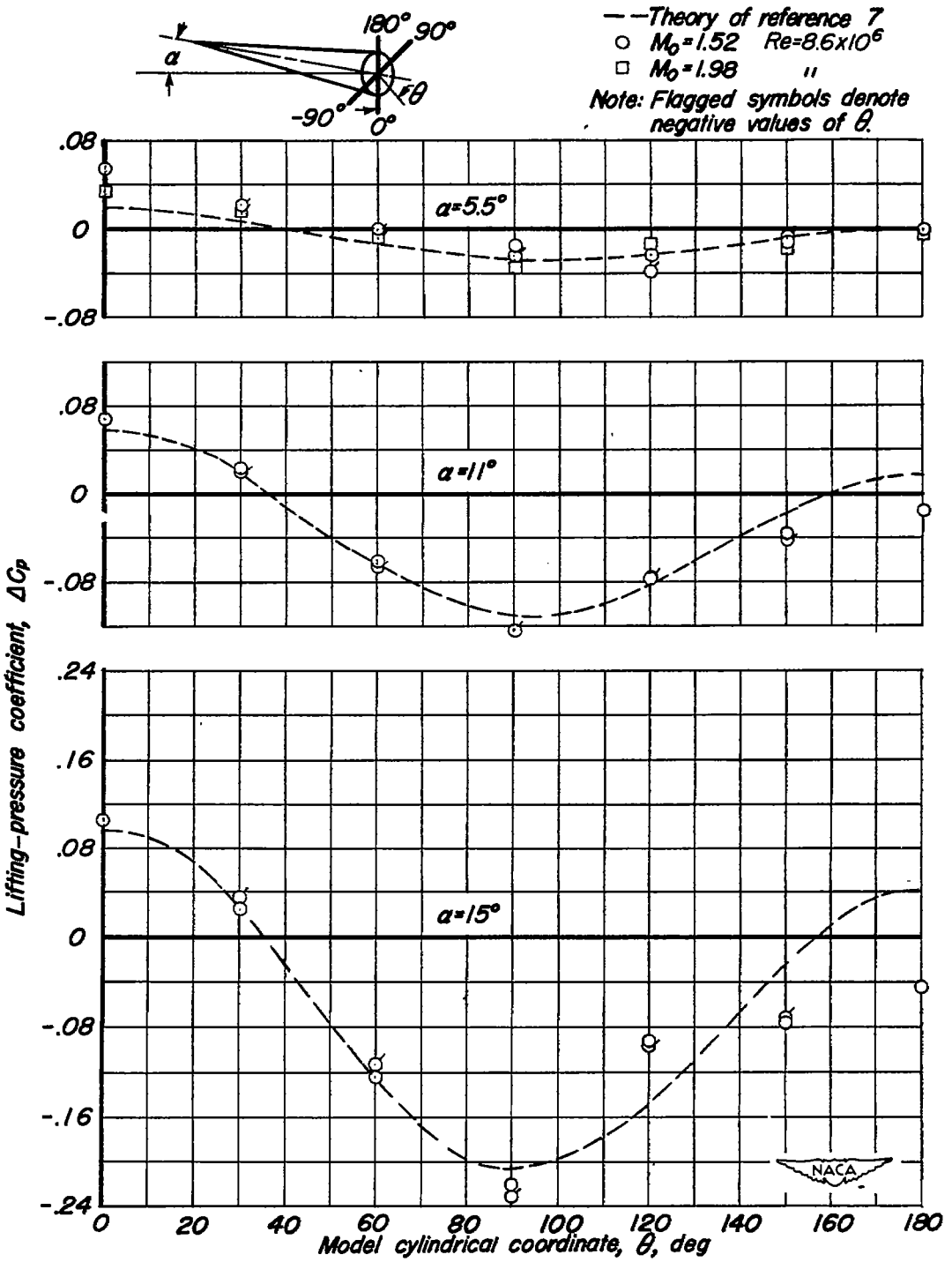

(c) Longitudinal station, $\frac{x}{L} = 0.492$.

Figure 3.- Continued.

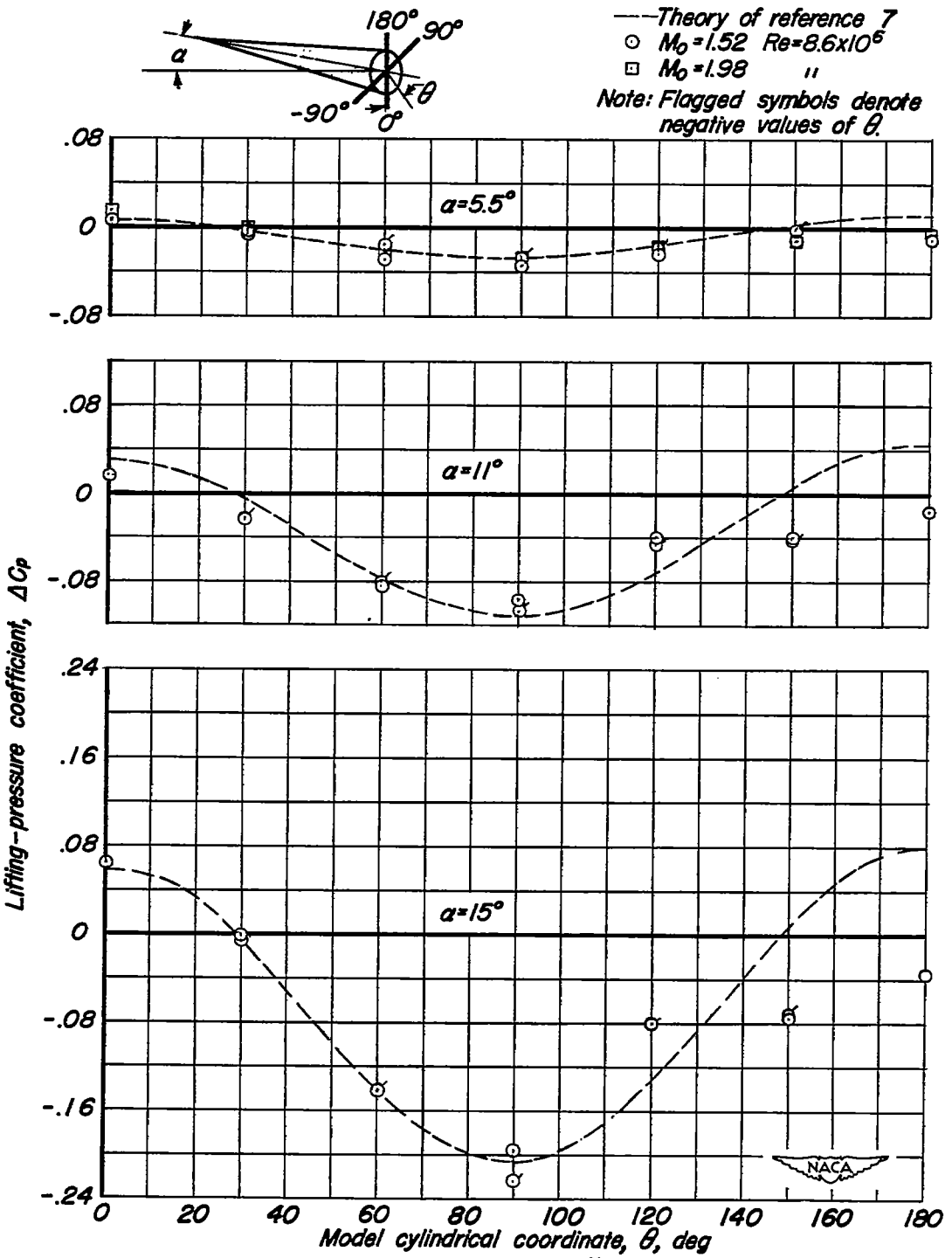

(d) Longitudinal station, $\frac{X}{L} = 0.655$.

Figure 3.– Continued.

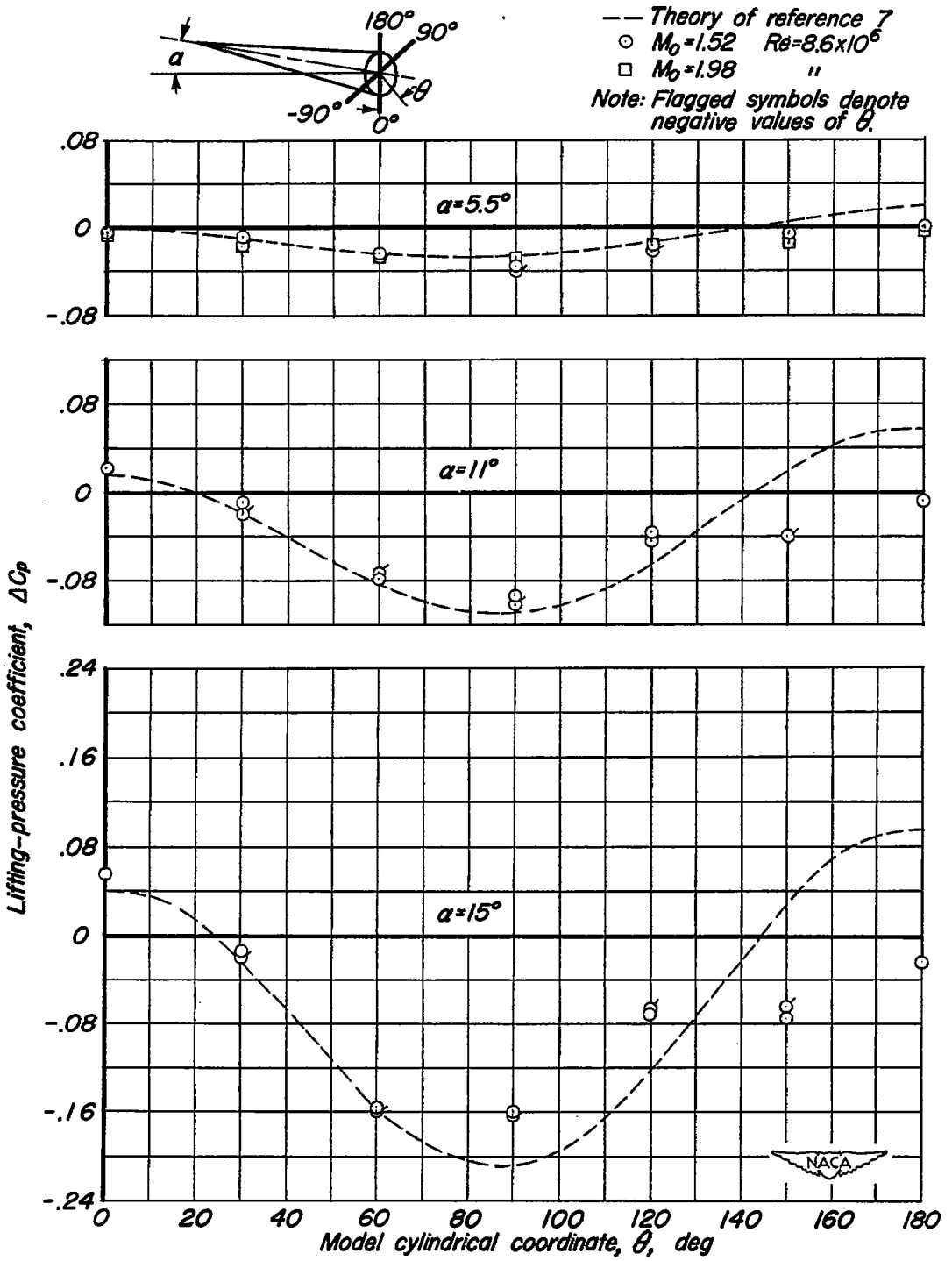

(e) Longitudinal station, $\frac{X}{L}$=0.737.

Figure 3.- Continued.

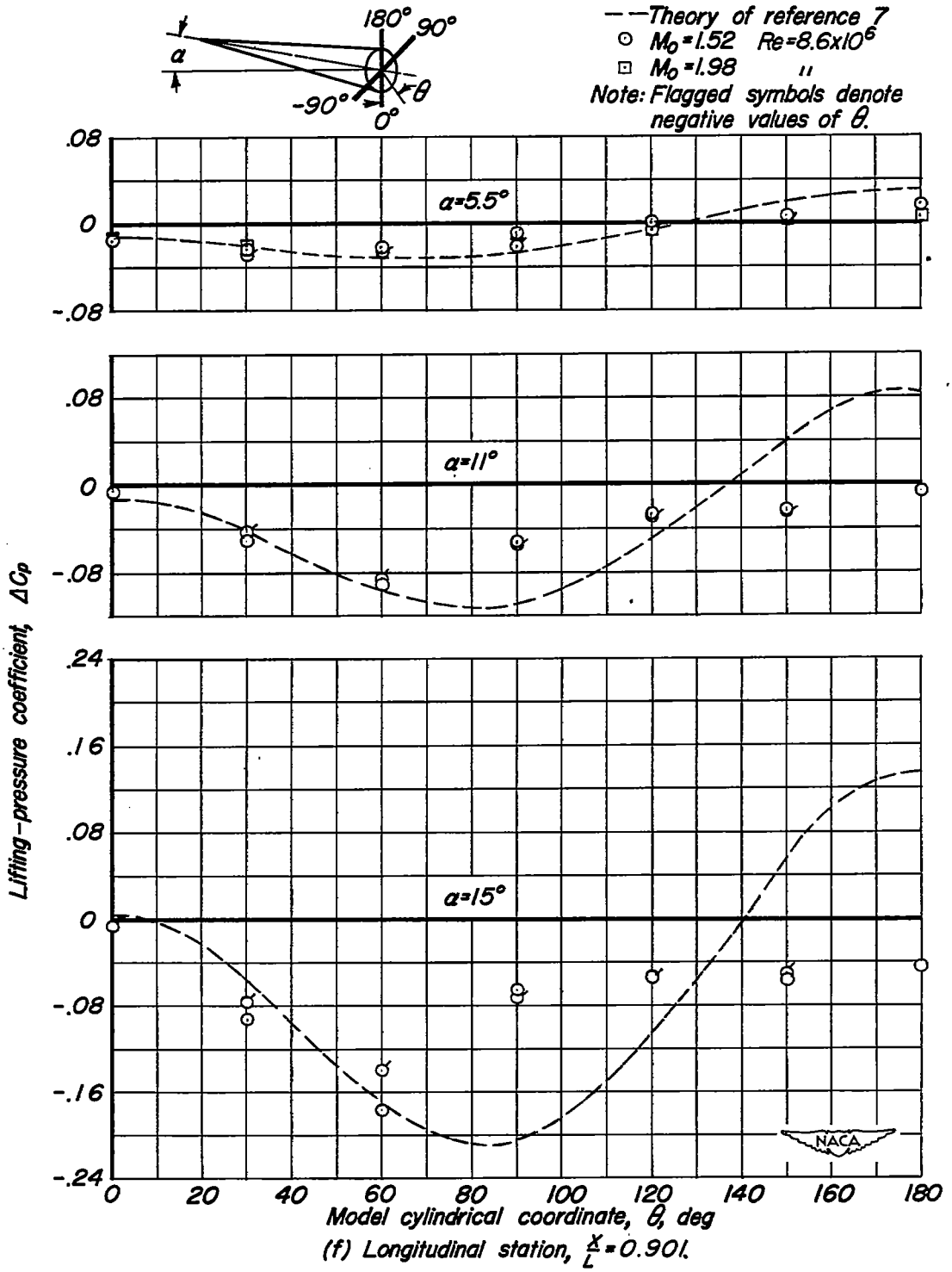

(f) Longitudinal station, $\frac{x}{l}$ = 0.90l.

Figure 3.– Concluded.

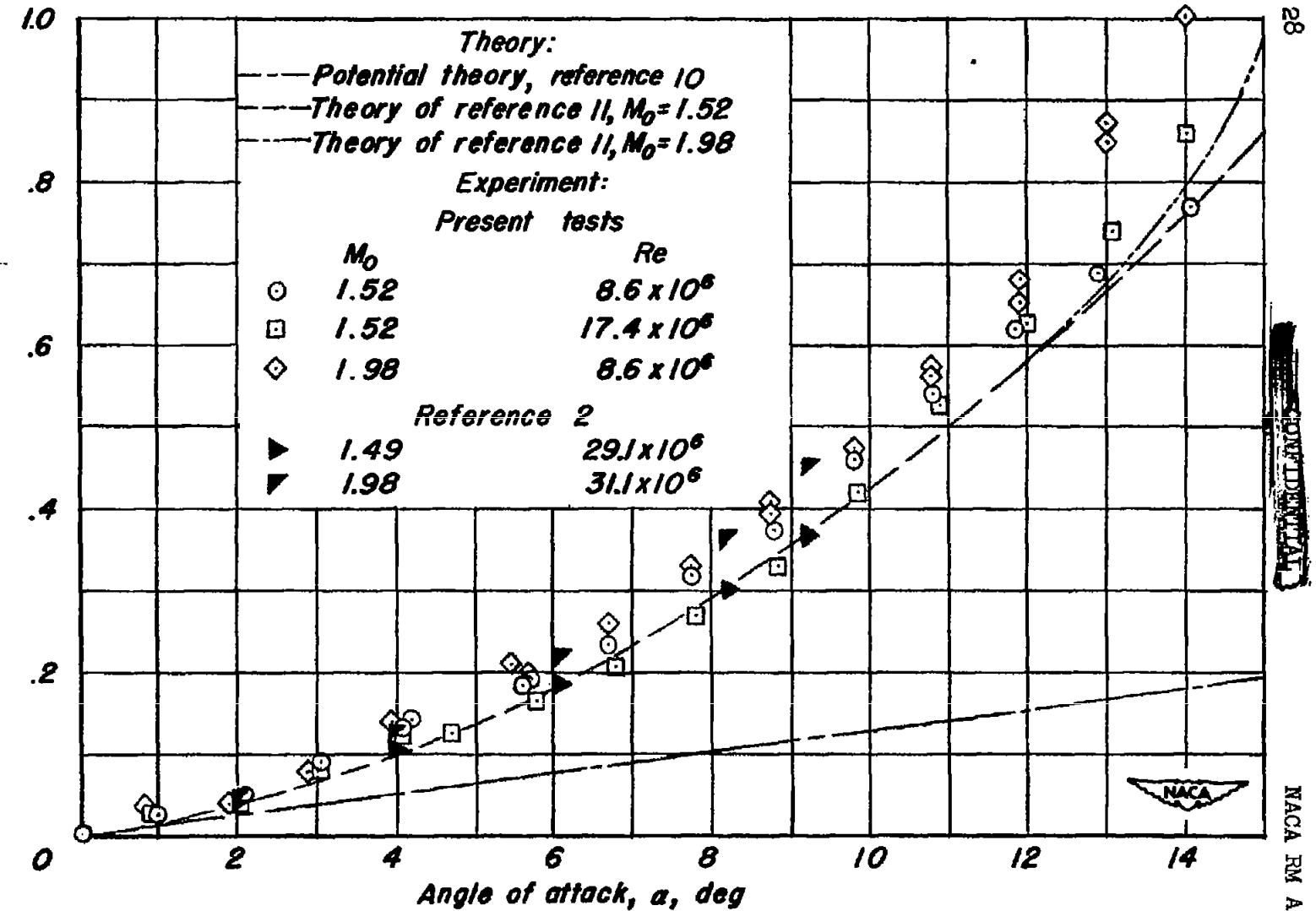

Figure 4.- Variation of lift coefficient with angle of attack for the body.

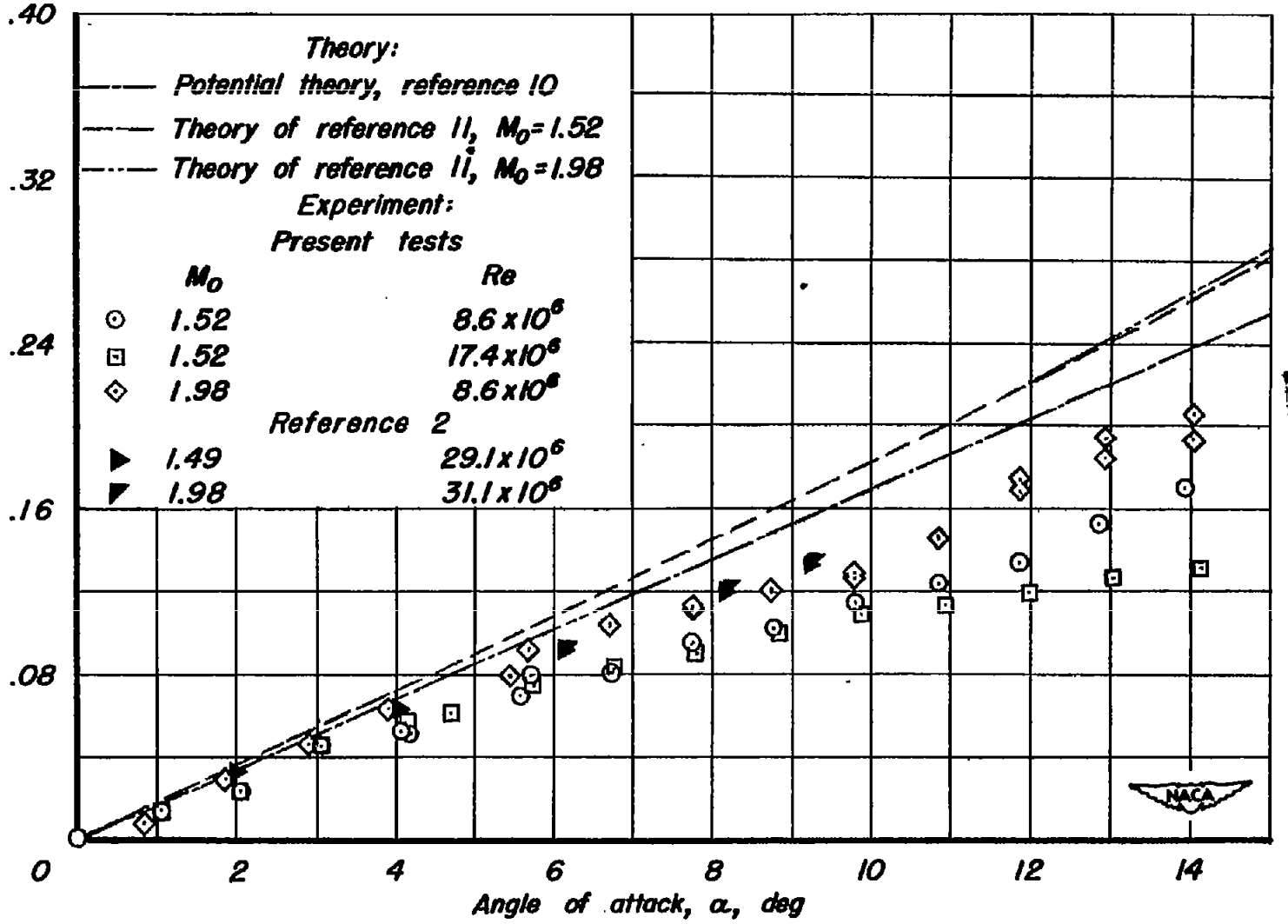

Figure 5.- Variation of pitching-moment coefficient with angle of attack for the body.

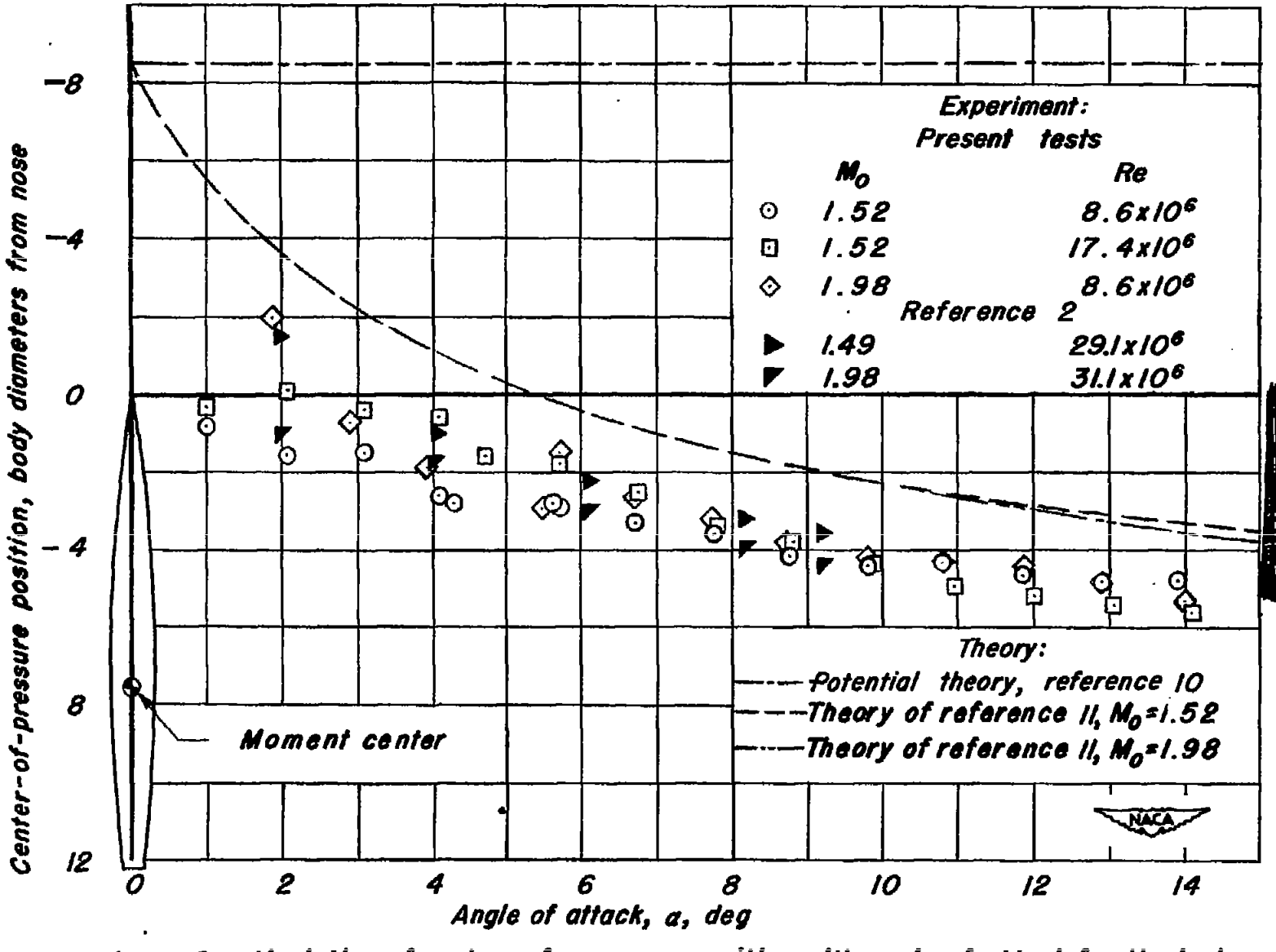

Figure 6.- Variation of center-of-pressure position with angle of attack for the body.

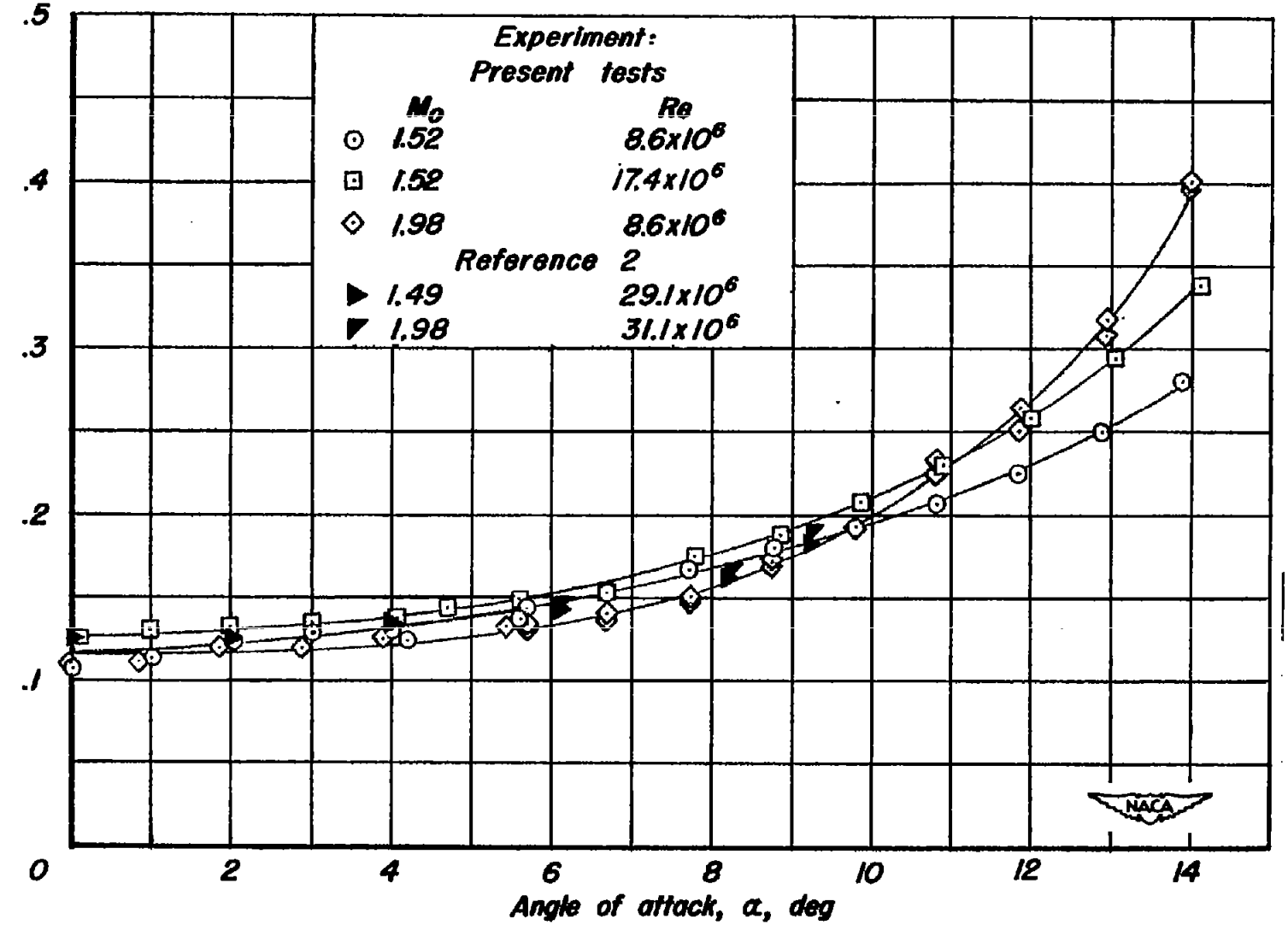

Figure 7.- Variation of foredrag coefficient with angle of attack for the body.

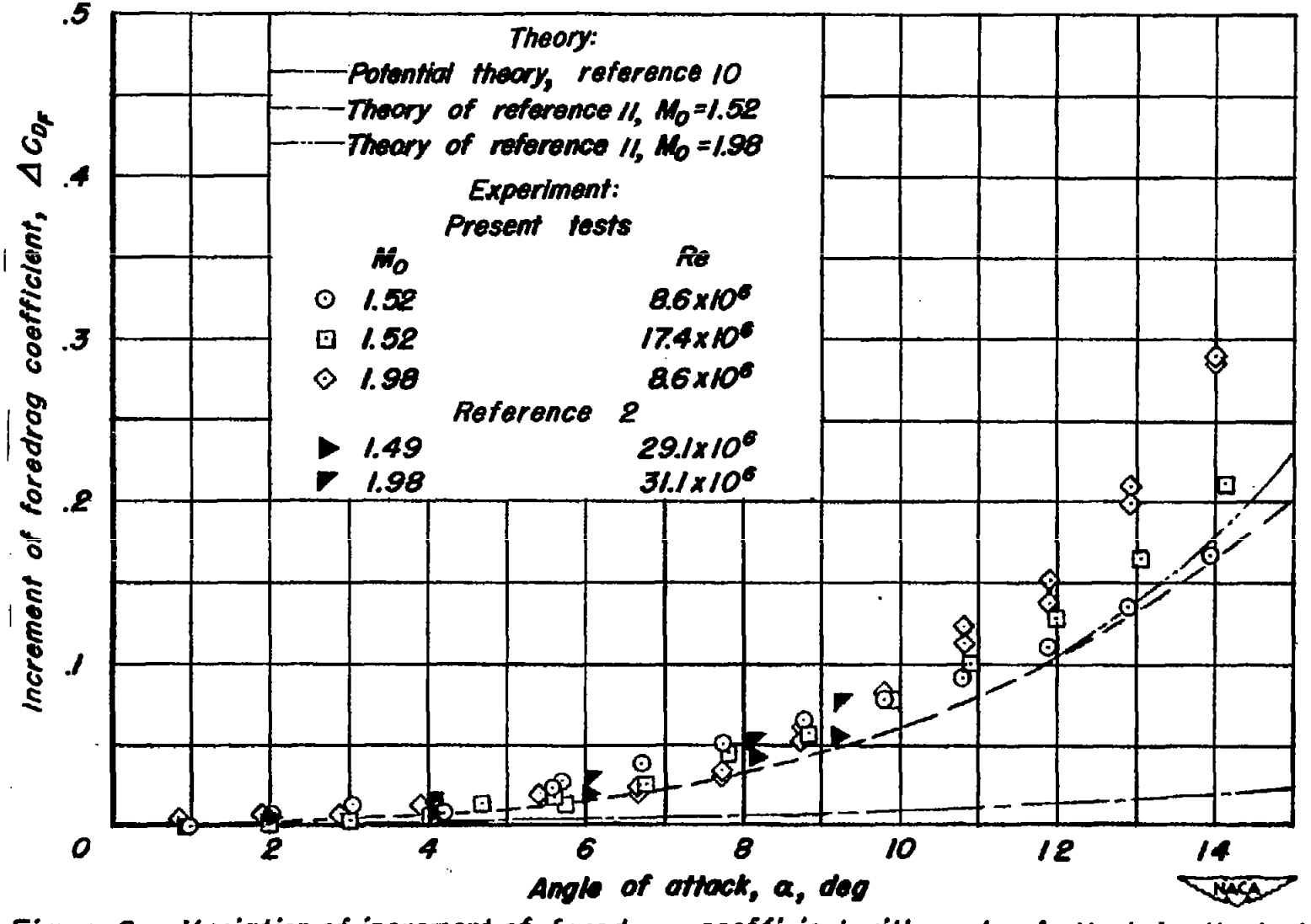

Figure 8.— Variation of increment of foredrag coefficient with angle of attack for the body.

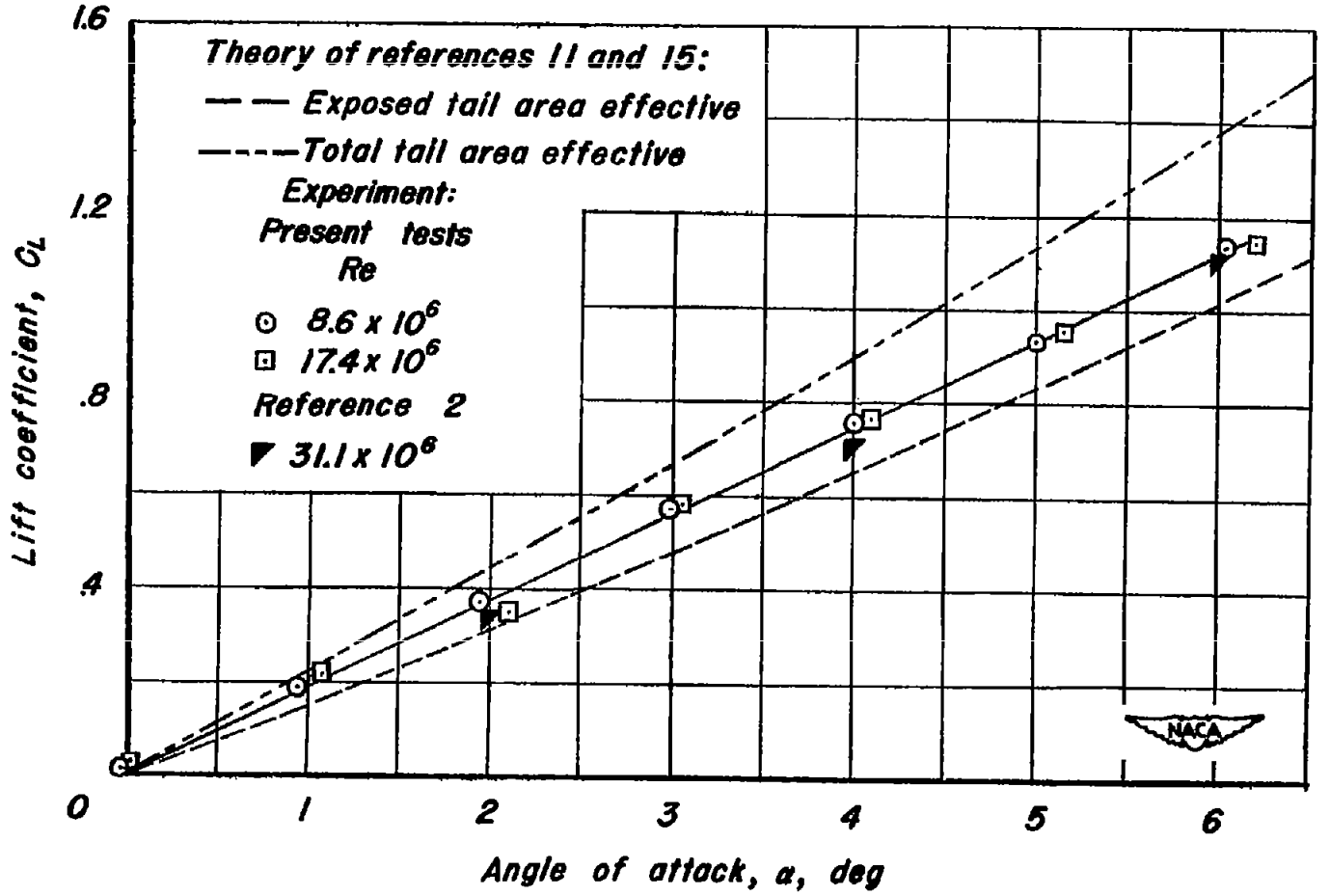

Figure 9. —Variation of lift coefficient with angle of attack for the body–tail combination at a Mach number of 1.98.

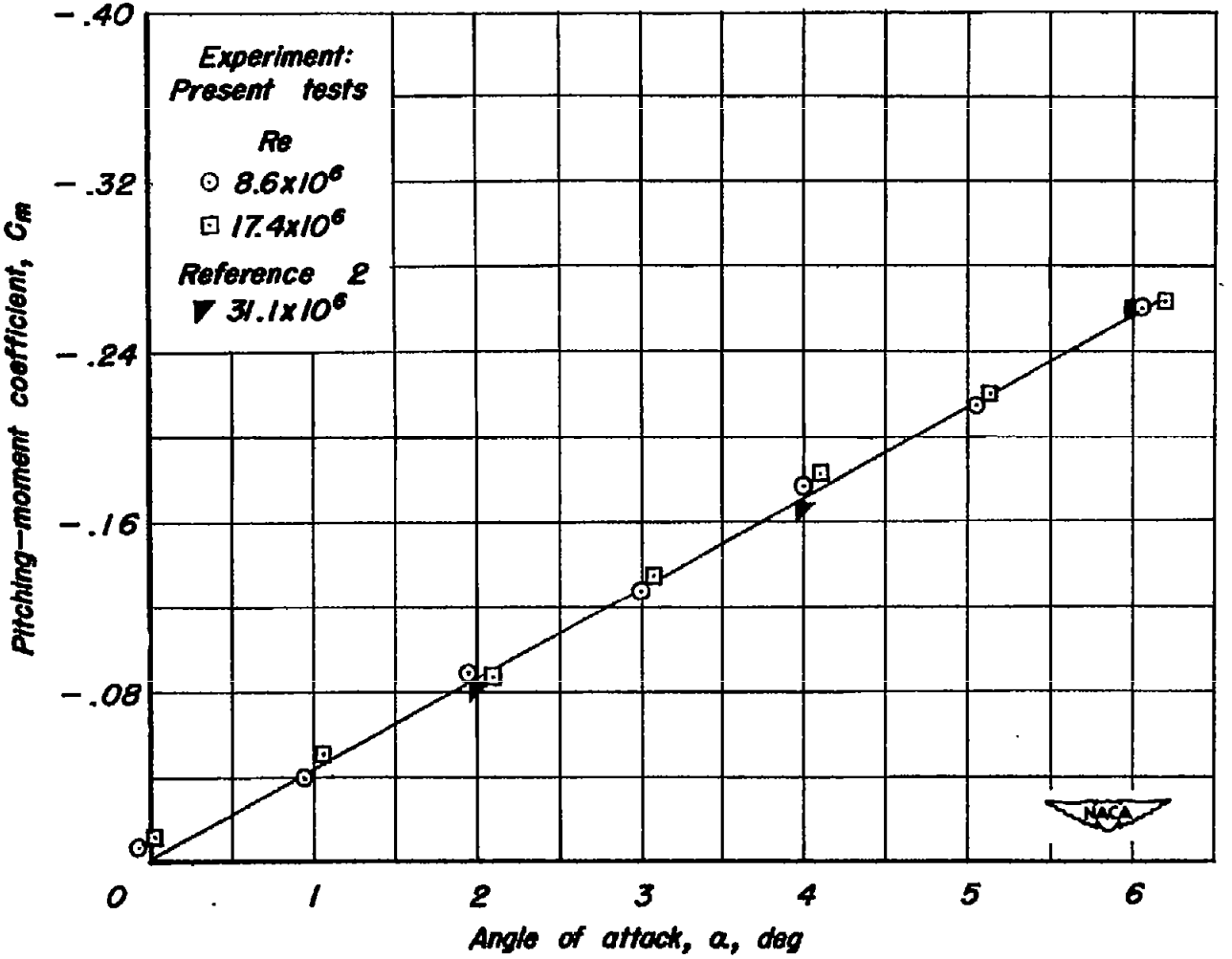

Figure 10.—Variation of pitching-moment coefficient with angle of attack for the body-tail combination at a Mach number of 1.98.

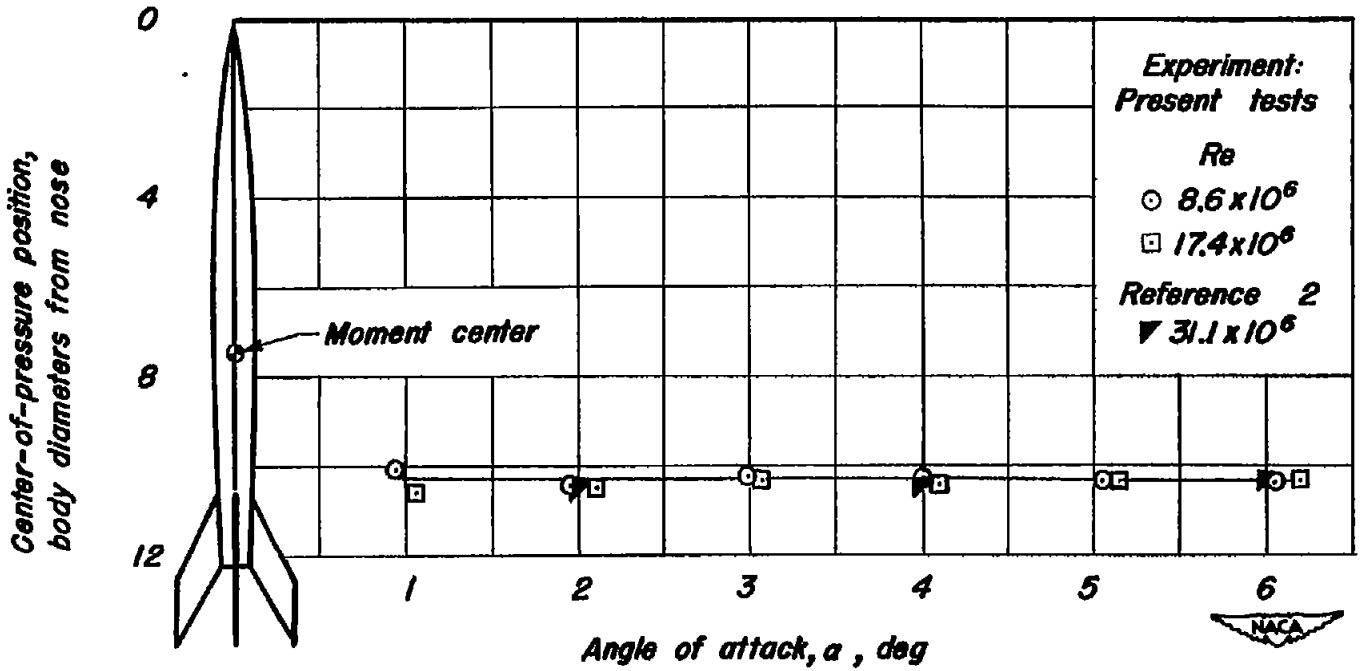

Figure 11.— Variation of center-of-pressure position with angle of attack for the body-tail combination at a Mach number of 1.98.

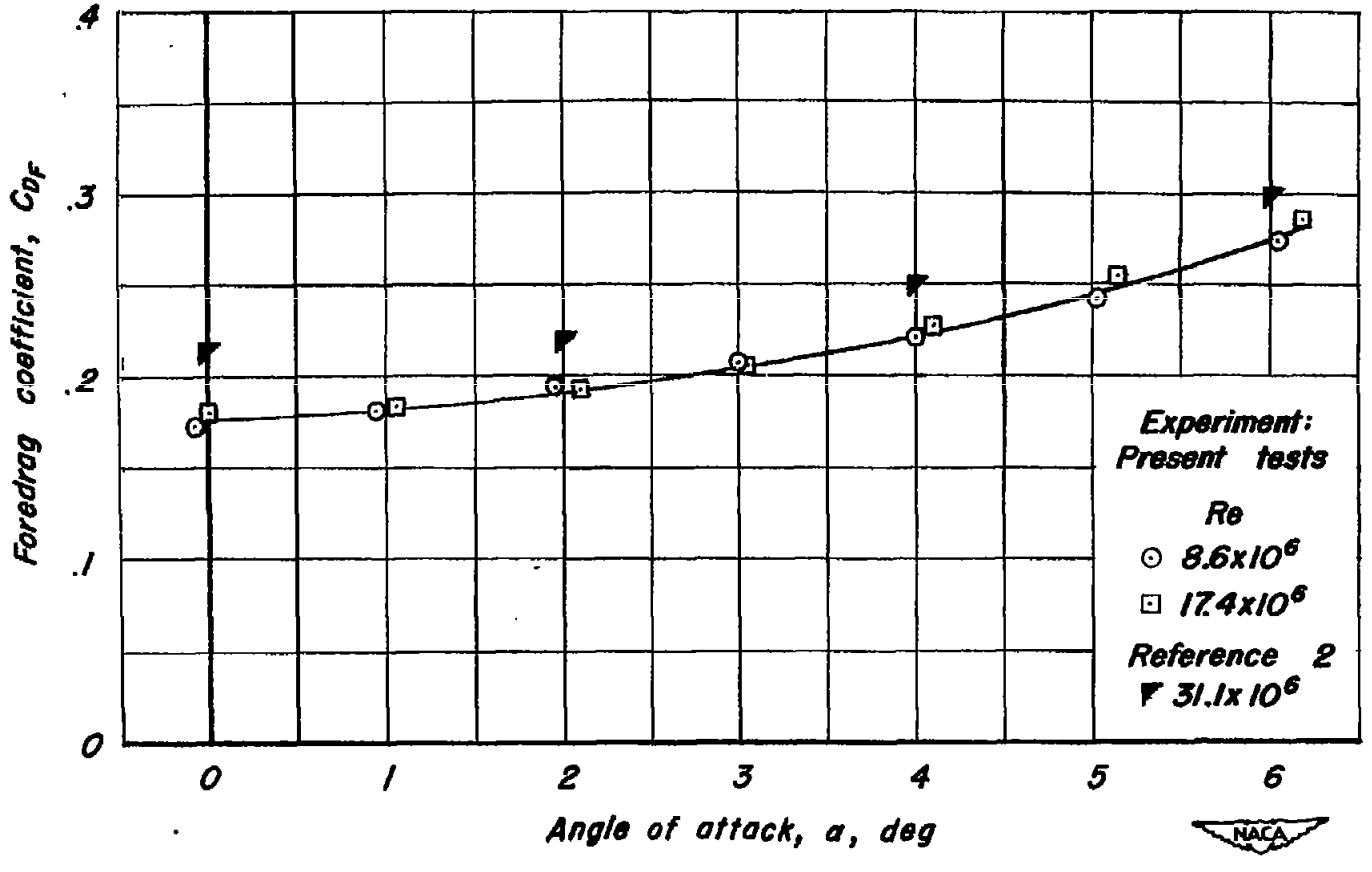

Figure 12.—Variation of foredrag coefficient with angle of attack for the body–tail combination at a Mach number of 1.98.

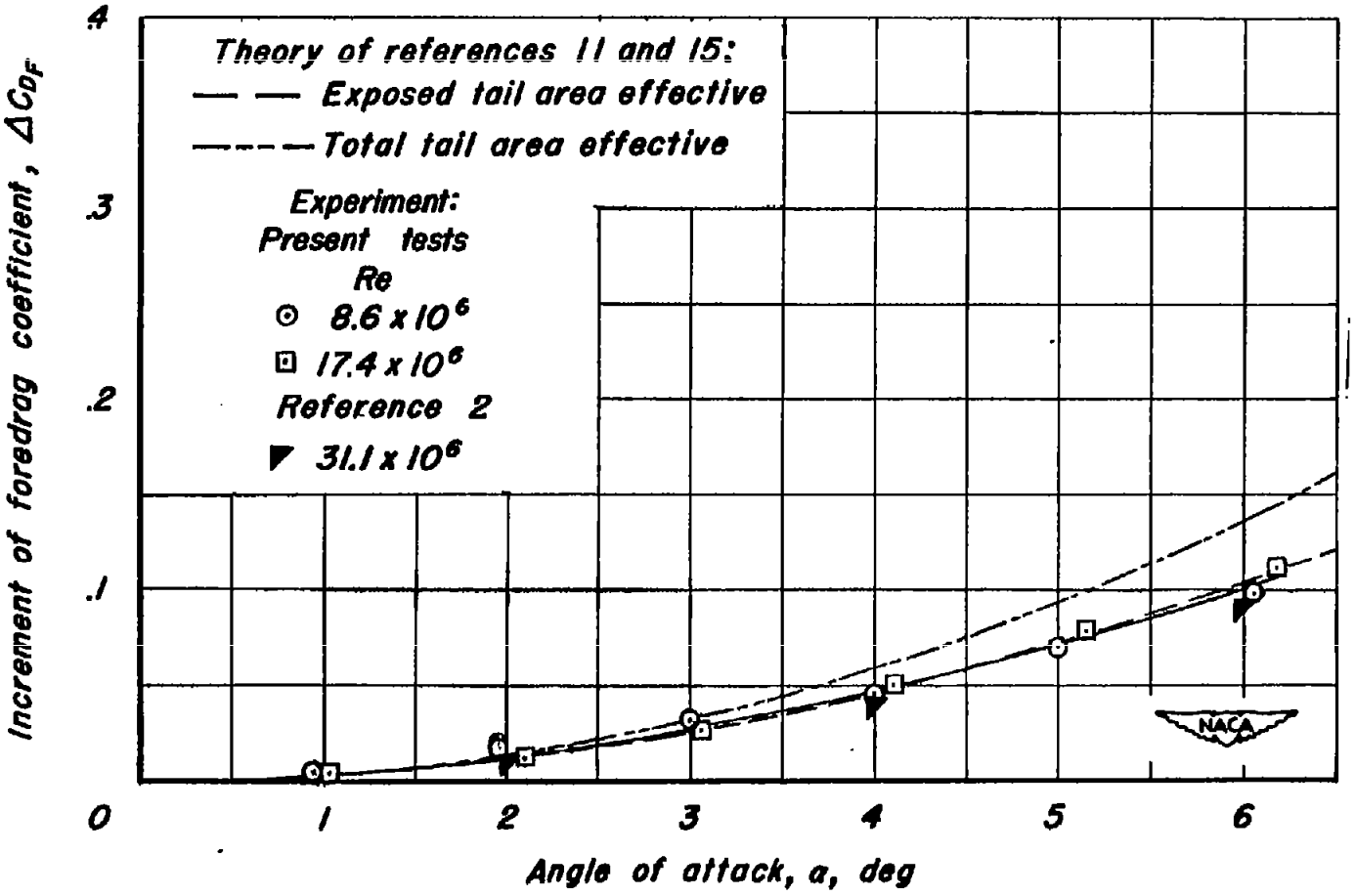

Figure 13.- Variation of increment of foredrag coefficient with angle of attack for the body-tail combination at a Mach number of 1.98.